SCIENTIFIC REPORTS

OPEN

SUBJECT AREAS:
ELECTROCATALYSIS
FUEL CELLS

Received
23 September 2014

Accepted
21 November 2014

Published
10 December 2014

Correspondence and requests for materials should be addressed to H.L.T. (thln@whut.edu.cn)

* These authors contributed equally to this work.

CeO_2 nanocubes-graphene oxide as durable and highly active catalyst support for proton exchange membrane fuel cell

M. Lei[1,2]*, Z. B. Wang[3,4]*, J. S. Li[3], H. L. Tang[3], W. J. Liu[1] & Y. G. Wang[2]

[1]State Key Laboratory of Information Photonics and Optical Communications, Beijing University of Posts and Telecommunications, Beijing 100876, China, [2]School of Science, Beijing University of Posts and Telecommunications, Beijing 100876, China, [3]State Key Laboratory of Advanced Technology for Materials Synthesis and Processing, Wuhan University of Technology, Wuhan 430070, China, [4]Institut für Funktionelle Grenzflächen (IFG), Karlsruher Institut für Technologie, Hermann-von-Helmholtz-Platz 1, 76344 Eggenstein-Leopoldshafen, Germany.

Rapid degradation of cell performance still remains a significant challenge for proton exchange membrane fuel cell (PEMFC). In this work, we develop novel CeO_2 nanocubes-graphene oxide nanocomposites as durable and highly active catalyst support for proton exchange membrane fuel cell. We show that the use of CeO_2 as the radical scavenger in the catalysts remarkably improves the durability of the catalyst. The catalytic activity retention of Pt-graphene oxide-8 wt.% CeO_2 nanocomposites reaches as high as 69% after 5000 CV-cycles at a high voltage range of 0.8–1.23 V, in contrast to 19% for that of the Pt-graphene oxide composites. The excellent durability of the Pt-CeO_2 nanocubes-graphene oxide catalyst is attributed to the free radical scavenging activity of CeO_2, which significantly slows down the chemical degradation of Nafion binder in catalytic layers, and then alleviates the decay of Pt catalysts, resulting in the excellent cycle life of Pt-CeO_2-graphene oxide nanocomposite catalysts. Additionally, the performance of single cell assembled with Nafion 211 membrane and Pt-CeO_2-graphene oxide catalysts with different CeO_2 contents in the cathode as well as the Pt-C catalysts in the anode are also recorded and discussed in this study.

Proton exchange membrane fuel cell (PEMFC), the most promising energy conversion device, has attracted considerable attention because of its high efficiency, high power density, and zero pollutant emission[1–5]. However, the rapid degradation of cell performance still remains a significant challenge prior to the commercial applications of PEMFC[4]. The poor cycle life of PEMFC mainly originates from the degradation of key materials including proton exchange membrane (PEM) and catalytic electrode[6–8]. Perfluorosulfonic acid ionomers such as Nafion is commonly used as PEM and catalyst binder in PEMFC. The use of perfluorosulfonic acid ionomers in PEMFC is critical for the establishment of proton transport pathway in the fuel cell. However, the chemical degradation of perfluorosulfonic acid ionomers in PEMFC is frequently observed in fuel cells after a long period of operation[9].

Numerous studies have revealed that the instability of Nafion during fuel cell operation was mainly ascribed to the attack of free radicals such as hydroxyl and hydroperoxyl radicals[10–12]. The radicals are easily produced in PEMFC through the reaction of hydrogen and oxygen on the electrode or the decomposition of hydrogen peroxide in the presence of metal ion contamination in membrane[11]. The free radical attack can lead to the formation of pinholes or cracks in membrane, which in turn results in gas crossover and ultimately the failure of the fuel cell. Additionally, the dissolution of Nafion binder in catalytic layers also causes the loss of catalytic layers and leads to the rapid degradation of electrocatalytic activity and cell performance. Although it is critical to prevent the degradation of the Nafion binder, there are few existing strategies which enable the efficient stabilization of Nafion binder in the catalyst. It has been shown that CeO_2 nanoparticles could be used as effective free radical scavengers in PEM to slows down the chemical degradation of membrane[9,11,12]. However, the chemical dissolution of Nafion binder in catalytic layers still remains problematic since the free radicals are mainly produced at the surface of catalytic electrode and then the newly-generated radical may first attack the Nafion

binder. Development of a radical scavenging catalytic electrode will be of great importance for both cases, but so far the radical scavengers have only found very few applications in catalytic electrode.

With regard to catalytic electrode, the catalyst support plays an important role in the performance of the electrode[13]. Recently, graphene has attracted an increasing amount of interest for the use as catalyst support. However, the 2D graphene always tends to stack together due to the strong π-π interaction, which significantly inhibit various properties of graphene such as the effective supporting area for Pt catalysts[14]. Graphene oxide (GO) is the oxidation state of graphene, in which the hydrophilic groups such as carboxyl (–COOH) and hydroxyl (–OH) are introduced on the surface of graphene by strong oxidant[15,16], effectively preventing the restack of graphene. Metal oxides, which can be well dispersed on the grapheme oxide, have been used for the functionalization of grapheme oxide catalyst support. However, the previous studies mainly focused on enhancing the catalytic activity of GO supported Pt catalyst with the metal oxides[17–19]. The effect of the metal oxide addictive on the stability of the catalyst was rarely studied. Moreover, there were few reports on the fuel cell performance of the catalyst based on the GO/metal oxide. In this paper, we develop a novel Pt/CeO_2/GO catalyst eletrocatalyst, in which CeO_2 functions as the radical scavenger to improve the durability of the catalyst. The structure and morphology of CeO_2, GO, and the CeO_2–GO nanocomposites are analyzed by X-ray diffraction (XRD) and transmission electron microscopy (TEM). The performance of single cell assembled from Nafion 211 membrane and Pt/CeO_2/GO catalyst with different CeO_2 contents in the cathode are also recorded and discussed in this study. The results show that the Pt-CeO_2 nanocubes-GO nanocomposites exhibit pronounced electrocatalytic properties and the doping of CeO_2 in catalyst remarkably improves the durability of the electrocatalytic activity.

Results

The XRD patterns of CeO_2, GO and the CeO_2-GO nanocomposites with different CeO_2 content are recorded for structural characterization. As shown in Figure 1, the positions of diffraction peak collected from the CeO_2/grapheme oxide nanocomposites are fully consistent with the XRD patterns of CeO_2 and graphene oxide. No additional peak has been observed, indicating that the nanocomposites are composed of CeO_2 and graphene oxide. No impurity was incorporated during the recombination process. Furthermore, the increased relative intensity of diffraction peaks of CeO_2 and GO with increasing the content of CeO_2 indicated that the doping amount of CeO_2 in the nanocomposite can be precisely controlled with the designed process.

In order to get an overview on the morphology of the nanocomposites, TEM images (Figure 2) were taken from the nanocomposites with various CeO_2 contents. It is clear that a large graphene oxide layer can be observed from the image and the CeO_2 nanocubes with size of around 5 nm were homogeneously distributed at the surface of graphene oxide. It is also evident from the TEM images that the density of the CeO_2 nanocubes on the grapheme oxide can be finely controlled by varying the doping amount of CeO_2 during the synthesis.

The Pt nanoparticles were loaded onto the CeO_2-GO nanocomposites using the well-established polyol approach[20,21]. To investigate the activity of the Pt/CeO_2/Graphene oxide catalyst, the performance of single cell assembled from Nafion 211 membrane and Pt/CeO_2/Graphene oxide catalyst with different CeO_2 contents in the cathode were characterized in terms of polarization curve (Figure 3a) and power density (Figure 3b). It is well known that the voltage-current curves can be divided into three regions: low current density regions (0–200 mA cm^{-2}), intermediate current density region (300–1000 mA cm^{-2}), and high current density region (more than 1000 mA cm^{-2}). During the low current density region, the performance of cell is dominated by the catalytic electrode. From Figure 3a, it is apparent that the performance of single cell at low current density region slightly increased when small amounts of CeO_2 (5 wt% and 8 wt%) were doped into the catalyst. In contrast, further increase in doping amount of CeO_2 in the catalyst results in the decay of cell performance. The results obtained here show great consistency with the relationship of catalytic activity and CeO_2 fractions in the electrode, which confirms that large amount of CeO_2 will influence the catalytic activity and the performance of catalytic electrode is mainly affected by the catalytic electrochemical active surface area. Additionally, a pronounced concentration polarization is monitored in the cell with 15 wt% of doped CeO_2 when the current density is up to 800 mA cm^{-2}. It demonstrates that excessive amounts of hydrophilic CeO_2 can increase the water-absorbing ability of electrode,

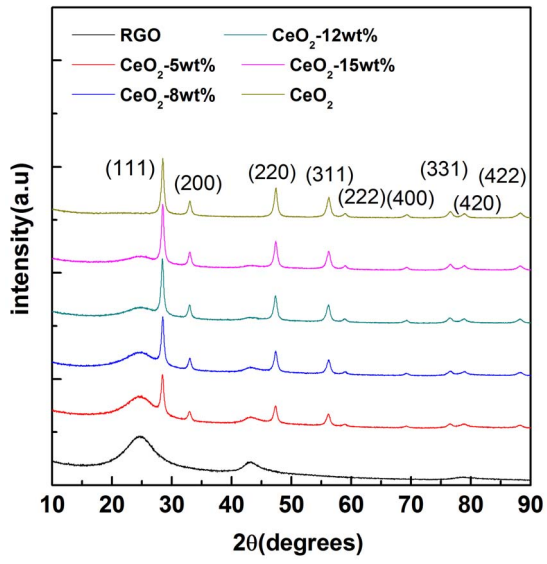

Figure 1 | XRD patterns of CeO_2, graphene oxide and the GO-CeO_2nanocomposites.

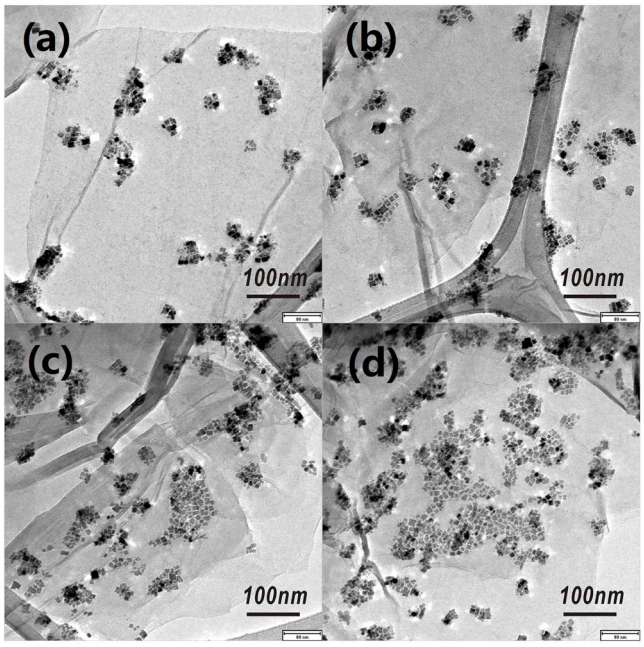

Figure 2 | High resolution TEM of the GO-CeO_2 nanocomposites with CeO_2 content of (a) 5wt%, (b) 8wt%, (c) 12wt% and (d)15wt%.

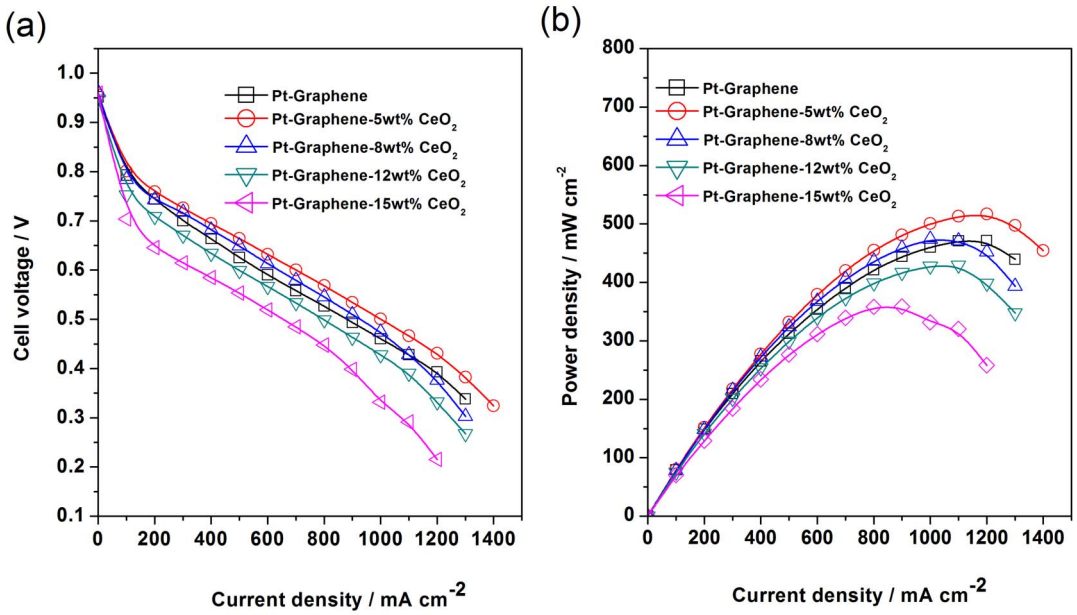

Figure 3 | (a) voltage–current performance and (b) power density of single cell assembled with $Pt/CeO_2/GO$ catalysts with different CeO_2 contents in the cathode.

resulting in the water-flooding in catalytic electrode, which in turn affects the gas transport and cell performance.

Figure 4 shows the open circuit voltage (OCV) degradation of single cells during 0.6–1.2 V voltage cycle. The OCV of the fuel cell assembled from Pt/graphene catalyst decreases significantly from 0.955 V to 0.895 V during 5000 cycles with an OCV reduction rate of 30.96 μV/cycle. The OCV for the fuel cell assembled from Pt/CeO_2/graphene oxide catalyst with CeO_2 of 5, 8, 12 and 15 wt% decreases to 0.932, 0.944, 0.945 and 0.948 V during the first 3100 minutes, respectively. The corresponding OCV degradation rate is about 11.87, 5.68, 5.16, and 3.61 μV/cycle, respectively, demonstrating that Pt/graphene catalysts with higher CeO_2 contents are more durable.

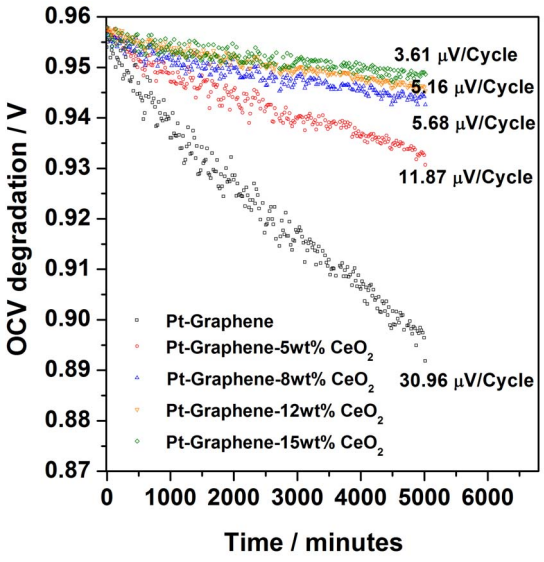

Figure 4 | Open circuit voltage (OCV) degradation of the single cell assembled with Pt/CeO_2/Graphene oxide catalysts with different CeO_2 contents in the cathode.

Discussion

To understand the high performance of the single cell assembled from Pt/CeO_2/Graphene oxide catalyst, electrochemical impedance spectra of cells assembled from Pt-graphene catalysts consisting of various amounts of CeO_2 were recorded. As shown in Figure 5, the first intersection point between the Z-axis and impedance spectra reflects the resistance of proton transportation. Since all the tested cells have the same membrane electrolytes, i.e. Nafion 211, they exhibit rather similar proton transportation resistance of about 0.0027 Ω. The diameter of the corresponding semi-circle reflects the resistance of charge transfer R_{ct}, which is directly related to exchange current density j_0 and can be expressed as[3]:

$$R_{ct} = RT/nFj_0. \quad (1)$$

Accordingly, the exchange current density values j_0 of applied Pt-Graphene catalysts with CeO_2 content of 0 wt%, 5wt%, 8 wt%, 12 wt%, and 15 wt% are calculated as 3.015, 3.459, 2.767, 2.735, and

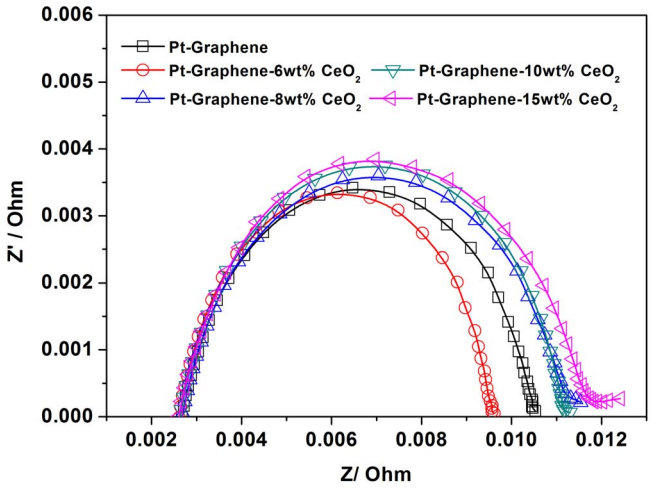

Figure 5 | Electrochemical impedance spectroscopy of the cell assembled with $Pt/CeO_2/GO$ catalysts with different CeO_2 contents in the cathode.

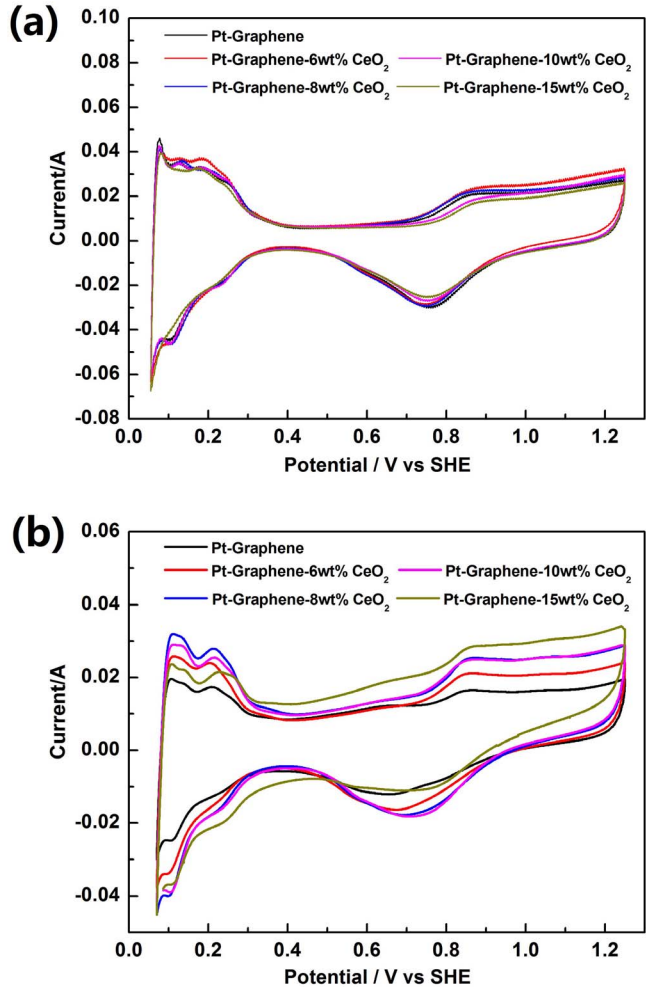

Figure 6 | Cyclic voltammograms of (a) single cell assembled with Pt/CeO_2/Grapheme as oxide reduction catalyst (before) and (b) after 5000 CV-cycles.

2.703 Acm^{-2}, respectively. Thus, it can be concluded that doping with 8 wt% of CeO_2 can improve the oxygen reduction capability of Pt-Graphene significantly. However, the activity of Pt-Graphene catalyst decreases with further increase of doping amount of CeO_2.

Cyclic voltammograms were applied to analyze the degradation of the fuel cells. The Pt/CeO_2/GO nanocomposites were fabricated by a pulse-microwave assisted polyol route with Pt content of ~40 wt%. The catalytic activity or electrochemical active surface area can be estimated by the value of charge transform calculated from the hydrogen oxidation peak observed from the cyclic voltammograms. Figure 6a shows the initial cyclic voltammograms of the cell assembled with Nafion 211 membrane and Pt/CeO_2/GO catalyst with different CeO_2 fractions in the cathode as well as the Pt/C catalyst (40wt%Pt, JM) in the anode. During the measurement, argon was fed into the working electrode (cathode: Pt/CeO_2/GO catalyst) and the hydrogen was fed into the counter and reference electrode (anode: Pt/C catalyst). With this configuration, the electrochemical active surface area obtained is mainly contributed by cathode catalytic layers. As shown in Figure 6a, the peaks assigned to the hydrogen adsorption and desorption on Pt surface at the position of −0.15 V vs SHE were clearly observed from all the catalysts with different amount of CeO_2. Additionally, the peak of oxygen reduction is also visible in the range of 0.98–0.75 V. The results demonstrate that the Pt nanoparticles were successfully deposited on the surface of CeO_2/GO nanocomposites and the doping of CeO_2 into the composite catalytic electrode cannot present toxicity to the catalytic activity of Pt catalyst. It is easy to draw a conclusion that the electrochemical active surface area slightly increased after a small amount doping of CeO_2. The reason can be attributed to the spillover of proton on the surface of CeO_2[12,22], which can assist the formation of new proton transport pathways, resulting in the increased three phase (proton, electron and reaction gas) interface area. Higher doping amount of CeO_2 will not help to improve the catalytic activity. Indeed, the electrochemical active surface area even decreased with the larger doped amount of CeO_2 in the catalyst layer since CeO_2 doesn't possess catalytic activity. Larger amount of CeO_2 doping can block the defect sites on the GO surface for the further deposition of Pt nanoparticles or block the active catalytic sites on the Pt catalysts.

Previous research results had shown that the free radicals could be produced in cathode by a two electron hydrogen-oxygen reaction during the high voltage condition in fuel cell[11]. Due to the presence of a large number of surface defects or primarily oxygen vacancies on the CeO_2 nanocubes, the CeO_2 could undergo redox reactions. Such redox process could be used for scavenging the free radicals. Therefore, we expect the introduction of CeO_2 nanocubes in the catalyst lead to the improved catalyst durability. In order to characterize the durability of the electrocatalytic activity of Pt/CeO_2/GO nanocomposites, the nanocomposite catalysts with different amounts of CeO_2 were assembled into the cathode of single cells which were operated in a high voltage region of 0.8–1.23 V. After 5000 CV-cycles, the cyclic voltammograms of all the nancomposite catalysts are presented in Figure 6b and the electrochemical active surface area (ECSA) of Pt/GO, Pt-GO-5wt% CeO_2, Pt-GO-8wt% CeO_2, Pt-GO-12wt% CeO_2 and Pt-GO-15 wt% CeO_2 were calculated to be 13.62, 43.30, 52.46, 49.07 and 34.23 m^2g^{-1}, respectively. The ECSA decreased by *ca*.81%, 45%, 31%, 34% and 53% for Pt/GO, Pt-GO-5wt% CeO_2, Pt-GO-8wt% CeO_2, Pt-GO-12wt% CeO_2 and Pt-GO-15 wt% CeO_2, respectively. It can be clearly seen that the doping of CeO_2 in the catalytic electrode remarkably improves the durability of the electrocatalytic activity. The catalytic electrode is normally prepared using Nafion as binder. Numerous studies found that the dissolution of Nafion binder could lead to the decay of Pt catalyst, resulting in a rapid degradation of the catalytic electrode[23–27]. The free radicals produced on the electron surface may first attack the Nafion binder and then destroy the electrode structure. Due to this reason, the activity surface area of Pt/GO significantly decreased 81% and the doping of CeO_2 does help to slow down the dissolution of binder and prolong the cycle life of catalytic electrode. Additionally, it is worthy to note that the catalytic activity retention of Pt-GO-8 wt% CeO_2 nanocomposites reached up to 69% after 5000 CV-cycles at a high voltage range of 0.8–1.23 V.

In summary, a novel CeO_2 nanocubes-GO nanocomposites with free radical scavenging capability was developed by a facile hydrothermal method and used as support for Pt catalysts in fuel cell. The XRD and TEM characterization confirmed that the CeO_2 nanocubes on the CeO_2 nanocubes-GO nanocomposites are highly crystalline and well dispersed at the surface of GO. The catalytic electrodes were prepared by a pulse-microwave assisted polyol route. The CV and cell performance were tested and the results show that a small amount of CeO_2 doping (<8%) can increase the electrochemical active surface area and improve the cell performances. The durability of the electrocatalytic activity of the nanocomposites was characterized using CV-cycles in a high voltage region of 0.8–1.23 V. The results demonstrate that the doping of CeO_2 could significantly slow down the dissolution of Nafion binder and prolong the cycle life of catalytic electrode. In the case of Pt-Grapheme oxide-8 wt.% CeO_2 nanocomposites, the catalytic activity retention reached 69% after 5000 CV cycles, in contrast to 19% for that of the Pt/GO composites.

Methods

Preparation of graphene oxide (GO) and CeO_2 nanocubes-GO nanocomposites. The GO was synthesized from natural graphite powder (99.95%). Briefly, 1 g of graphite, 0.8 g of $K_2S_2O_8$, and 0.8 g of P_2O_5 were added into 10 mL of concentrated

H_2SO_4 under strong stirring at 80°C for 6 h. After cooling down the solution to room temperature, 250 mL of deionized (DI) water was added into the above solution and aged for 12 h. The suspension was filtered, washed, and dried to obtain the black solid. After mixing the black solid with 60 ml of concentrated H_2SO_4 and 5 g of $KMnO_4$ in an ice bath, the suspension was transferred to a water bath and magnetically stirred at 35°C for 2 h. The resulting dark-brown paste was diluted with the slow addition of 150 ml of DI water and further stirred for another 2 h. 10 mL (30 wt%) of H_2O_2 was slowly added to quench the solution to produce a golden-brown solution. After the resultant product was centrifuged, the sample was washed with HCl (1 : 10) and DI water, respectively, until the pH of the washed solution was *ca.* 6. Finally, the product was dried at 40°C.

For synthesis of CeO_2 nanocubes-GO nanocomposites, 100 mg of GO was dissolved in 60 mL distilled water by ultrasonic dispersion for 2 h until a yellow-brown suspension was formed. 0.1 mmol of cerium (III) nitrate was then added into the suspension under vigorous stirring for another 2 h. After transfer the mixed suspension to a 100 mL Teflon-lined stainless-steel autoclave, 10 mL of toluene, 1.5 mL of oleic acid, and 0.1 mL ethylenediamine were added into the autoclave without stirring. Finally, the autoclave was sealed and put into a furnace with a temperature of 180°C for 24 h. The obtained black precipitates were washed with alcohol for several times and dried in vacuum for further characterization. The weight percentage of the CeO_2 nanocubes is 8% in the obtained CeO_2-GO composites in this case. CeO_2-GO composites with different CeO_2 contents was also prepared by by varying the amount of added GO during the synthesis. The weight percentage of CeO_2 nanocubes in the CeO_2-GO composites was controlled to be 5, 8, 12 and 15 wt%, respectively.

Synthesis of Pt-GO-CeO_2 catalysts. The Pt-GO-CeO_2 catalyst were prepared by a pulse-microwave assisted polyol route[20]. H_2PtCl_6 with Pt content of 0.15 g was first well mixed with ethylene glycol (EG, 100 mL) in a beaker by ultrasonic treatment for 30 min, and 0.35 g GO-CeO_2 was added into the mixture. The pH value of the mixed suspension was adjusted to 10 by drop-wisely addition of 1.0 mol L^{-1} NaOH/EG solution. After dispersing with high speed stirring and ultrasonication for 30 min, the Pt ions in the suspension were reduced to Pt^0 by intermittent microwave-heating with pulses every 5 s for three times. After the reduction, the pH value of the suspension was adjusted to 2 using 0.1 M HCl to promote the adsorption of Pt nanoparticles onto supports.

Preparation of the membrane electrode assemblies. The resulting electrocatalyst powders were filtered, washed and dried at 80°C for 10 h in a vacuum oven. Membrane electrolyte assembly were prepared as follows[28]: firstly, catalyst inks were prepared by mixing the catalyst, 5 wt% Nafion solution (DuPont D520) and isopropyl alcohol with a weight ratio of 1 : 6 : 10 under vigorous stirring. Then the catalyst slurry was screen printed onto the GDL (TGP-060, Toray Inc.) to form the electrocatalyst layer. Pt loading was 0.2 mg cm^{-2} and 0.4 mg cm^{-2} for the anode and the cathode, respectively. The catalyst layer was dried at 60°C for 10 min and at 90°C in N_2 atmosphere for 3 min. The Nafion 112 membrane (50 μm) and electrocatalyst layers were bonded together by hot pressing under 10 MPa at 125°C for 90 s.

Characterization of the catalysts. Transmission electron microscopy (TEM) was carried out on a JEOL 6300 at an accelerating voltage of 100 kV. The samples for these measurements were dispersed in absolute ethanol by vibration in the ultrasonic pool. The solutions were dropped onto a copper grid coated with amorphous carbon films and dried in air before the performance.

Single fuel cell was assembled with the as-prepared MEAs and graphite flow field plates under the pressure of 10 MPa. The active area of the cell was 2×2 cm^2. H_2 and air were used as fuel and oxidant without back pressure. The flow rates of H_2 and air were 300 sccm and 2000 sccm, respectively. Cell performances were recorded by a Solartron 1260. The MEA was mounted in a single cell test fixture with a serpentine flow field and a fuel cell clamp (with an active area of 2×2 cm^2). The single cells were first activated using a cycling protocol. The cell was operated at each pre-set current density for 2 minutes with the increment of 50 mA cm^{-2}. At the maximum current density where the output voltage is greater than 0.3 V, the cell was continuously operated for 2 h and then back to OCV in 50 $mAcm^{-2}$ increments with operation of cell for 2 minutes at each step. The process was repeated until the performance reached a stable state at each testing point. After the activation, the single cell performance was assessed. A stoichiometry ratio of 1.5 and 2.5, for H_2 and air respectively, was used for the test.

The electrochemical active surface area or activity of the cell was estimated from cyclic voltammegrams (CV) measured with a scan rate of 20 mV/s at ambient temperatures. During the measurement, hydrogen at a flow rate of 10 sccm was fed to the anode (which served as the counter and reference electrodes) and argon to the cathode at 100 sccm, which served as working electrode. The potential was scanned between 0.05 V and 1.2 V. Electrochemical active surface areas were obtained by comparing the area of hydrogen oxidation peaks from the cyclic voltammograms. Electrochemical accelerated durability tests were employed to evaluate the long-term performance of catalysts. During the tests, the CV cycles were conducted between 0.6 and 1.2 V versus dynamic hydrogen electrode (anode).

1. Wang, C. *et al.* Multimetallic Au/FePt3 Nanoparticles as Highly Durable Electrocatalyst. *Nano Lett.* **11**, 919–926 (2011).
2. Fujigaya, T. & Nakashima, N. Fuel Cell Electrocatalyst Using Polybenzimidazole-Modified Carbon Nanotubes As Support Materials. *Adv. Mater.* **25**, 1666–1681 (2013).
3. Wang, G. *et al.* Pt Skin on AuCu Intermetallic Substrate: A Strategy to Maximize Pt Utilization for Fuel Cells. *J. Am. Chem. Soc.* **136**, 9643–9649 (2014).
4. Zhang, S. *et al.* A review of accelerated stress tests of MEA durability in PEM fuel cells. *Int. J. Hydrogen Energ.* **34**, 388–404 (2009).
5. Wang, Z. B. *et al.* Balancing dimensional stability and performance of proton exchange membrane using hydrophilic nanofibers as the supports. *Int. J. Hydrogen Energ.* **38**, 4725–4733 (2013).
6. Wang, Z. B., Tang, H. L. & Pan, M. Self-assembly of durable Nafion/TiO2 nanowire electrolyte membranes for elevated-temperature PEM fuel cells. *J. Membr. Sci.* **369**, 250–257 (2011).
7. Tang, H. L., Pan, M. & Wang, F. A mechanical durability comparison of various perfluocarbon proton exchange membranes. *J. Appl. Polym. Sci.* **109**, 2671–2678 (2008).
8. Tang, H. L. *et al.* Highly durable proton exchange membranes for low temperature fuel cells. *J. Phys. Chem. B* **111**, 8684–8690 (2007).
9. Wang, Z. *et al.* Synthesis of Nafion/CeO2 hybrid for chemically durable proton exchange membrane of fuel cell. *J. Membr. Sci.* **421**, 201–210 (2012).
10. Cheng, Y. T., Tang, H. L. & Pan, M. A strategy for facile durability improvement of perfluorosulfonic electrolyte for fuel cells: Counter ion-assisted decarboxylation at elevated temperatures. *J. Power Sources* **198**, 190–195 (2012).
11. Dowding, J. M. *et al.* Cerium oxide nanoparticles scavenge nitric oxide radical ((NO)-N-center dot). *Chem. Commun.* **48**, 4896–4898 (2012).
12. Wang, X. *et al.* Ceria-based nanocomposite with simultaneous proton and oxygen ion conductivity for low-temperature solid oxide fuel cells. *J. Power Sources* **196**, 2754–2758 (2011).
13. Tang, J. *et al.* Tailored design of functional nanoporous carbon materials toward fuel cell applications. *Nano Today* **9**, 305–323 (2014).
14. Si, Y. & Samulski, E. T. Exfoliated Graphene Separated by Platinum Nanoparticles. *Chem. Mater.* **20**, 6792–6797 (2008).
15. Toelle, F. J., Gamp, K. & Muelhaupt, R. Scale-up and purification of graphite oxide as intermediate for functionalized graphene. *Carbon* **75**, 432–442 (2014).
16. Rao, F., Deng, S., Chen, C. & Zhang, N. Graphite oxide-supported Karstedt catalyst for the hydrosilylation of olefins with triethoxysilane. *Catal. Communi.* **46**, 1–5 (2014).
17. Jiang, L. H. *et al.* Controlled Synthesis of CeO2/Graphene Nanocomposites with Highly Enhanced Optical and Catalytic Properties. *J. Phys. Chem. C* **116**, 11741–11745 (2012).
18. Yu, S. P. *et al.* Graphene-CeO2 hybrid support for Pt nanoparticles as potential electrocatalyst for direct methanol fuel cells. *Electrochim. Acta* **94**, 245–251 (2013).
19. Chen, H. L. *et al.* One step synthesis of Pt/CeO2-graphene catalyst by microwave-assisted ethylene glycol process for direct methanol fuel cell. *Mater. Lett.* **126**, 9–12 (2014).
20. Tang, H. & Jiang, S. P. Self-Assembled Pt/Mesoporous Silica-Carbon Electrocatalysts for Elevated-Temperature Polymer Electrolyte Membrane Fuel Cells. *J. Phys. Chem. C* **112**, 19748–19755 (2008).
21. Meng, H. & Shen, P. K. Tungsten carbide nanocrystal promoted Pt/C electrocatalysts for oxygen reduction. *J. Phys. Chem. B* **109**, 22705–22709 (2005).
22. Oh, T.-S., Boyd, D. A., Goodwin, D. G. & Haile, S. M. Proton conductivity of columnar ceria thin-films grown by chemical vapor deposition. *Phys. Chem. Chem. Phys.* **15**, 2466–2472 (2013).
23. Xie, J., Wood, D. L., More, K. L., Atanassov, P. & Borup, R. L. Microstructural changes of membrane electrode assemblies during PEFC durability testing at high humidity conditions. *J. Electrochem. Soc.* **152**, A1011–A1020 (2005).
24. Xie, J., Wood, D. L., Wayne, D. M., Zawodzinski, T. A., Atanassov, P. & Borup, R. L. Durability of PEFCs at high humidity conditions. *J. Electrochem. Soc.* **152**, A104–A113 (2005).
25. Kongkanand, A. *et al.* Degradation of PEMFC Observed on NSTF Electrodes. *J. Electrochem. Soc.* **161**, F744–F753 (2014).
26. Zhang, S. S. *et al.* A review of platinum-based catalyst layer degradation in proton exchange membrane fuel cells. *J. Power Sources* **194**, 588–600 (2009).
27. Xu, F., Fitzwater, D. & Xie, J. Degradation Investigation of Nafion Ionomer Network In Catalyst Layers Durability and Diagnostics: Catalyst Layers. *ECS Trans.* **41**, 673–678 (2011).
28. Tang, H. L., Wang, S. L., Jiang, S. P. & Pan, M. A comparative study of CCM and hot-pressed MEAs of PEM fuel cells. *J. Power Sources* **170**, 140–144 (2007).

Acknowledgments

This work was financially supported by The Program for New Century Excellent Talents in University (NCET-13-0684, NCET-12-0911), Fund of State Key Laboratory of Information Photonicsand Optical Communications (Beijing University of Posts and Telecommunications,PR China), National Natural Science Foundation ofChina (Grant No. 61376018, 51102019, 51272031, 51472187, 51272200).

Author contributions

H.L.T. and M.L. conceived the idea, analyzed the data and wrote the paper; Z.B.W. and J.S.L. performed the electrochemical experiments and wrote the paper; W.J.L. and Y.G.L. contributed to the corresponding synthesis and performed the characterization.

Additional information

Competing financial interests: The authors declare no competing financial interests.

How to cite this article: Lei, M. *et al.* CeO_2 nanocubes-graphene oxide as durable and highly active catalyst support for proton exchange membrane fuel cell. *Sci. Rep.* **4**, 7415; DOI:10.1038/srep07415 (2014).